

Synthesis and Evaluation of Polyacrylamide Based Filter Pellets Incorporating GAC, Iron Oxide, Zinc Oxide, and Kaolin for Chromium and Nickel Water Remediation



Mustapha Chabane^{1,2*}, Chikh Melkaoui³, Nacer Ferrah², Riad Mansour², Khaled Rahoui¹,
Benamar Dahmani¹

¹ University Centre of Naama, Naama 45000, Algeria

² Laboratory of Research on Spectrochemistry and Structural Pharmacology, Department of Chemistry, Science Faculty, University of Tlemcen, Tlemcen 13000, Algeria

³ Center for Scientific and Technical Research in Physical and Chemical Analysis (CRAPC), PO Box 384 Bousmail, Tipaza 42004, Algeria

Corresponding Author Email: chabane@cuniv-naama.dz

Copyright: ©2024 The authors. This article is published by IIETA and is licensed under the CC BY 4.0 license (<http://creativecommons.org/licenses/by/4.0/>).

<https://doi.org/10.18280/rcma.340212>

ABSTRACT

Received: 25 December 2023

Revised: 25 March 2024

Accepted: 8 April 2024

Available online: 29 April 2024

Keywords:

filter, carbon, iron oxide, zinc oxide, kaolin

The objective of this research is to manufacture new filter pellets based on polyacrylamide (PAM) activated carbon (GAC), iron oxide (Fe₂O₃), zinc oxide (ZnO) and kaolin and to evaluate their effectiveness in removing chromium and nickel from water. The synthesized filter pellets were characterized by FTIR, XRD and X-ray fluorescence. The XRF validation method would involve known amounts of chromium and nickel being retained by the filter pellets. The application of XRF gave precise measurements of the concentrations of Cr(VI) and Ni(II) fixed in the filter pellets. It was found that the values of the retention rates of Cr(VI) ions are higher in comparison with Ni(II) ions. The inclusion of inorganic additives influences the ability of filter pellets (FP) to retain Cr(VI) and Ni(II). FP2 (ZnO) showed reduced retention for both ions in comparison to FP1 (Fe₂O₃) and FP3 (Kaolin). FP3 (Kaolin) displayed better retention capacities for Cr(VI) and Ni(II) ions. The conductometric approach was also used to evaluate the retention of ions by the filter pellets. Comparing the conductivity of the feed solution with that of the filtered solution and the comparison between the different materials provided information on the most effective filter pellets for this purpose.

1. INTRODUCTION

Human survival depends on water, which is considered the second most important life essential after air. However, human activities, such as wasteful usage, have negatively impacted the quality of water worldwide. Although the United Nations has recognized the human right to clean water, many people suffer from the lack of it; a significant number of people still lack access to clean water. According to the World Water Council, the situation is predicted to worsen as an estimated 3.9 billion people are expected to live with limited water resources by 2030 [1, 2]. Environmental protection has become a major economic and political issue because all countries of the world are concerned with the safeguarding of freshwater resources. Currently, industrial water discharges containing relatively large amounts of metallic substances constitute a growing problem. Their presence in effluents poses a threat to any biological organism [3]. Hexavalent chromium (Cr(VI)) is categorized as a Group 1 carcinogen and can cause cancer through various intricate mechanisms. It results in cellular harm by elevating oxidative stress, causing breaks in chromosomes, and forming DNA adducts [4]. Nickel is found in the

environment through natural sources and human activities, and its role as a trace element for animals and humans is not fully recognized. Industrial processes, fuel use, and waste disposal can lead to nickel pollution, which can cause various health problems, including mitochondrial dysfunction and oxidative stress. Recent research suggests that nickel exposure can lead to epigenetic alterations that can potentially cause cancer. This review discusses the chemical characteristics of nickel in humans, its toxicity mechanisms, and environmental remediation strategies such as phytoremediation and phytomining [5]. The development of organic-inorganic hybrid materials may provide a solution for the water industry's quality and quantity problems caused by climate conditions and contamination, as these materials have been shown to effectively remove toxic compounds from wastewater [6]. Hybrid materials made from clay minerals treated with amino group-containing molecules are popular for their unique properties and many uses. Modified versions have demonstrated exceptional adsorption capabilities [7]. Iron, zinc, and silica materials are used for eco-friendly water depollution due to their effectiveness in removing contaminants like heavy metals and organic compounds. Metal oxide nanoparticles, especially transition metal oxides,

are promising materials with potential benefits in various fields including water purification [8]. Iron oxide nanoparticles are reactive and can remove pollutants through adsorption and chemical reactions. Iron oxide nanoparticles have become a popular choice as additives in polymeric membranes. They're popular in polymeric membranes for their effectiveness in removing arsenic and copper and can also improve the membrane's stability [9]. Zinc-based materials, like Zinc oxide nanorods can remove pollutants through photocatalysis. Polymer ZnO composite membranes can also prevent membrane fouling. Latest research proposes using ZnO nanoparticles to enhance polymeric membranes for wastewater treatment. However, research needs to address ZnO nanoparticle aggregation and leaking, study antifouling mechanisms, and conduct long-term application research [10]. Silica-based materials, such as mesoporous silica nanoparticles, have high specific surface area and pore volume, which enhances their adsorption capacity. It has been demonstrated that the incorporation of silica can improve the effectiveness of water treatment. Through the utilization of silica fume and microwave heating, a mesoporous silica material was produced and found to be effective in eliminating Cu²⁺, Pb²⁺, and Cd²⁺ within the pH range of 5.0-7.0 [11]. Kaolinite is a clay mineral with eco-friendly properties, high surface area, and stability. It is used for environmental decontamination despite its low cation exchange and poor adsorption selectivity. Its properties can be improved through modification methods. Kaolinite-based nanomaterials are used for environmental decontamination, such as pollutant degradation and heavy metal adsorption [12]. Using inorganic materials for water depollution is a sustainable solution for environmental remediation. African palm fruit activated carbon is an effective material for removing heavy metals from wastewater in Nigeria, especially at 80°C for 60 minutes. This suggests that it could be a solution for heavy metal pollution [13]. The production of affordable and sustainable GACs from waste materials for water treatment shows potential. Waste-based GACs can replace expensive non-renewable sources, but more research is required to optimize their production and understand their performance in continuous bed columns and regeneration potential [14]. High molecular weight acrylamide-based polymers are effective and cost-efficient adsorbents for heavy metal removal due to their enhanced adsorption efficiency. PAM is the most studied and commonly used organic polymer flocculent due to its wide applicability and cost-effectiveness. PAM combined with organic/inorganic matter can effectively remove heavy metals from contaminated water, with various potential industrial and environmental applications. A new flocculant, polyacrylamide-glutathione, was synthesized to trap cadmium, and its characteristics and application conditions in water bodies were analyzed. The obtained product had a high cadmium removal rate, and its primary mechanisms of flocculation were identified [15]. PAM and its modification with nanoclay have been the subject of recent research in this area, aimed at enhancing its adsorption properties for eliminating Ni²⁺ and Co²⁺. The results showed that PAM/Na-MMT nanocomposites were more efficient in adsorbing heavy metal ions than PAM and nanoclay, with a removal rate of 87.40% to 94.50% [16]. Mixed filters made of organic and inorganic materials can be an interesting way to purify water, as natural substances can improve membrane performance. These filters can treat water sources. In order to obtain an adequate form of mixed

mixtures applied for filtration tests in the laboratory, scientists prepared filter pellets in the form of discs. of which we can cite the research work of Park et al., 2007 prepared pellets based on cream for the diesel treatment [17]. In water treatment plants, the design of toxic substance elimination systems consists of the installation of cartridge filters containing either granular activated carbon or granular activated carbon combined with other organic or inorganic materials [18]. PAM has the ability to function as an additive, which is attributed to its capacity to easily combine with inorganic materials through the reactivity of the amide group. The research work aims to improve the elimination efficiency by proposing a new approach using a combination of organic and inorganic materials for sustainable water filtration. By filling these gaps, research contributes to the development of more efficient and environmentally friendly water purification solutions. In this context, filter pellets for sustainable water filtration was prepared using materials such as PAM, activated carbon, iron oxide, zinc oxide, and kaolin. The pellets were characterized using analytical techniques such as FTIR, XRD, and XRF. The effectiveness of the pellets in removing Cr(VI) and Ni(II) from water will be assessed through batch adsorption experiments examining various parameters. The development of sustainable solutions for water filtration will be contributed to by this research.

2. MATERIAL AND METHODS

2.1 Chemical reagents

In the study, Table 1 lists the technical information regarding the chemical reagents that were utilized to produce the filter pellets.

Table 1. Technical and commercial data of chemical products

Reagents	Commercial Name	Suppliers
(C ₃ H ₅ NO) _n	Polyacrylamide	Sigma Aldrich
Fe ₂ O ₃	Iron Oxide	Sigma Aldrich
ZnO	Zinc Oxide	Sigma Aldrich
Kaoline	K512	Sigma Aldrich
Granular Activated carbon	Filtrisorb200	Calgo carbon corporation
K ₂ Cr ₂ O ₇	Potassium dichromate	Sigma Aldrich
Ni(NO ₃) ₂ ·6H ₂ O	Nickel(II)nitrate hexahydrate	Sigma Aldrich
HNO ₃	Nitric acid	Sigma Aldrich
HCl	Hydrochloric acid	Sigma Aldrich
NaOH	Sodium hydroxide	Sigma Aldrich

2.3 Activated carbon treatment stage

2.3.1 Purification and activation of carbon

Activated carbon obtained from Indo Germán Carbón Limited in Cochin, with particle size 12 × 40 (mesh), iodine number 850 mg/g, effective size 0.55 to 0.75 mm, apparent density 0.38 g/cc, moisture content 2% was used in the study. The GAC was washed with 0.5M NaOH and 0.5M HCl solutions, followed by distilled water. The resulting washed carbon was dried. A portion of GAC was treated with nitric acid to undergo surface oxidation. The oxidation process involved refluxing acid-washed activated carbon with HNO₃ and distilled water for four hours, filtering, and repeating the

process. The resulting nitric acid-oxidized granular activated carbon was filtered, washed, dried. This process consists of combustion of activated carbon to increase the adsorption capacity by oxidizing contaminants from the interaction effect with air such as CO₂ or humidity. The degree of burn off was used to assign the granular activated carbon (GAC) that was prepared, and this calculation was done as follows [19, 20].

$$BO(\%) = \frac{W_{in} - W_{Fin}}{W_{in}} \times 100 \quad (1)$$

where, BO(%): Degree of burnoff; W_{in} : Initial weight (g); W_{Fin} : Final weight (g).

The BO(%) of GAC used for the experimental test is 9.5%.

2.4 Methodology for the manufacture of filter pellets

The mixture of Polyacrylamide, activated carbon, iron oxide, zinc oxide, and kaolin was prepared in specified proportions. Distilled water and acetone were added as solvents. The mixture was thoroughly stirred until it became cohesive, and filter discs (4 cm × 4 mm) were manufactured using a manual press with hydraulic pressure of 20 tons, then dried at a specific temperature (Figure 1). The mass percentages of the components are detailed in Table 2. It is important to note that achieving a compact structure involved conducting numerous trials.

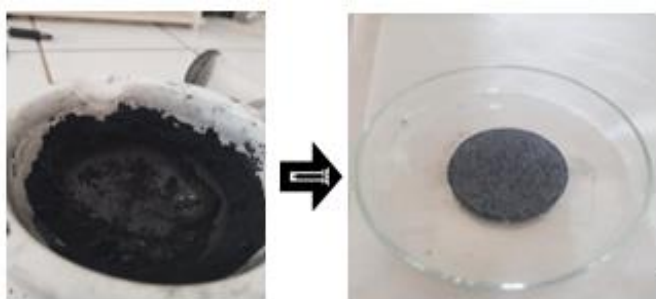


Figure 1. The experimental part involves the preparation of the mixing and filters discs

Table 2. Composition of filter pellets

Filter Pellets	PAM (%)	GAC (%)	Fe ₂ O ₃ (%)	ZnO (%)	Kaolin(%)
FP1	20	20	60	0	0
FP2	20	20	0	60	0
FP3	20	20	0	0	60

2.5 Technical characterization

2.5.1 Fourier transformed infrared spectroscopy (FTIR)

The samples of each filters pellets were dried at 50°C in a hot air oven for 24 h, and then a mixture of these samples and KBR pellets was prepared. The mixture was analyzed using a FTIR spectrophotometer (Spectrum, Perkin Elmer, USA) within the wave number range of 4000 to 400 cm to obtain spectral analysis. In each case, the average of 30 scans was represented by one spectrogram.

2.5.2 X-ray diffraction pattern analysis

The AXS Bruker D8 model, which is equipped with a

CuK α source ($\lambda=154$ nm), was used to establish the XRD diffractograms of the filter pellets. The diffraction angles (2θ) were measured between 5° to 90° under a potential difference of 40 kV and a lamp current intensity of 30 mA.

2.6 Filtration procedure

For the filtration study, nickel and chromium ion solutions were prepared at A setup comprising a vacuum pump connected to a conical flask, which holds a Buchner-style funnel with filtering pellets, is used to filter 250ml of the heavy metal solutions (Figure 2). The resultant filtered solution or permeate is gathered in an Erlenmeyer flask. All samples were kept in a freezer until analyzed, the filter disk is dried at a temperature of 90 degrees Celsius for 24 hours, and then the concentration of heavy metals (Cr, Ni) in the disk is measured before and after filtration.



Figure 2. Vacuum filtration assembly

2.7 Analytical methods

The concentration of nickel and chromium were determined using the Wavelength Dispersive X-ray Fluorescence Spectrometer (Bruker WDXRF S8 TIGER Series 2) in the filter disc samples. The XRF is equipped with an AG22 X-ray a concentration of 100 ppm of chromium (III) and nickel (II) ions were prepared from the analytical grade of K₂Cr₂O₇ and Ni (NO₃)₂.6H₂O salts. This was achieved through successive dilution of stock solutions of chromium (VI) and nickel with a concentration of 1000 ppm. The preparation method of the stock solution involves dissolving 2.829 grams of K₂Cr₂O₇ and 0.159 grams of Ni(NO₃)₂.6H₂O in 1 liter of doubly distilled water. The pH of the standard solution is 6.5, equivalent to the predominant species of CrO₄²⁻ with a chromium oxidation state of +6, as indicated by various confirmed researches. The pH of the standard nickel solution is 6.4. [21, 22]. tube with a Rh anode with a

maximum power of 4 kW and a current of up to 170 mA, a set of analysis crystals (XS-C, XS-55, PET, LiF(200), LiF(220)), proportional and scintillation detectors, collimators (0.17, 0.23, 0.46, and 1°), and Al and Cu filters of different thicknesses. Measurement and analysis conditions were selected using the Fundamental Parameters Method (FPM) by the Spectra plus software. The filter pellets samples are crushed, then 9 grams of licowax are mixed with 2 grams of sample powder. Pellets of the mixture are prepared by placing them in a pellet press at a pressure of 25 tons, and finally elemental analysis is conducted via XRF. All samples were measured as triplicates (n=3). The limit of detection for chromium is 5.5 ppm, and for nickel it is 4.4 ppm. The precision (CV) of the analysis is 0.95% for nickel and 2.06% for chromium.

2.8 Data processing

The retention rate of filter disc Ret, is determined as a percentage according to Eq. (2):

$$Ret(\%) = \frac{C_{Ret}}{C_{Feed}} \times 100 \quad (2)$$

where, Ret(%): Retention rate of filters pellets; C_{Ret} : Concentration of heavy metal retained by filters pellets (ppm); C_{Feed} : Concentration of heavy metal in feed solution, (ppm).

To calculate the rejection rates, the following equation was used:

$$R(\%) = \left(1 - \frac{\rho_{Permeate}}{\rho_{Feed}}\right) \times 100 \quad (3)$$

where, R(%): Rejection rate of filter pellets; $\rho_{permeate}$: Conductivity of permeate solution ($\mu\text{s}/\text{cm}$); ρ_{Feed} : Conductivity of feed solution ($\mu\text{s}/\text{cm}$).

3. RESULTS AND DISCUSSION

3.1 Manufacturing filter discs

Different methods of manufacturing filter discs (pellets) were tested.

For the first trial, a melange consisting of 33.33% powdered activated charcoal and 66.67% fixative (licowax C) was prepared and then placed in a pellet press with a pressure of 20 tonnes. Subsequently, the pellet was retrieved and left to dry for 1 hour at 150°C. A fragile filter disc that disintegrates upon contact with water was obtained.

For the second trial, 8g of licowax were mixed with 100ml of acetone in a beaker at room temperature with agitation to obtain a solution (S1). Then, 50% zinc oxide and 50% powdered activated charcoal were placed in a mortar and mixed, adding drops of solution S1 to achieve a homogeneous paste. The same procedures as the first trial were followed for manufacturing the filter discs, resulting in a fragile membrane that is less hard and disintegrates upon contact with water.

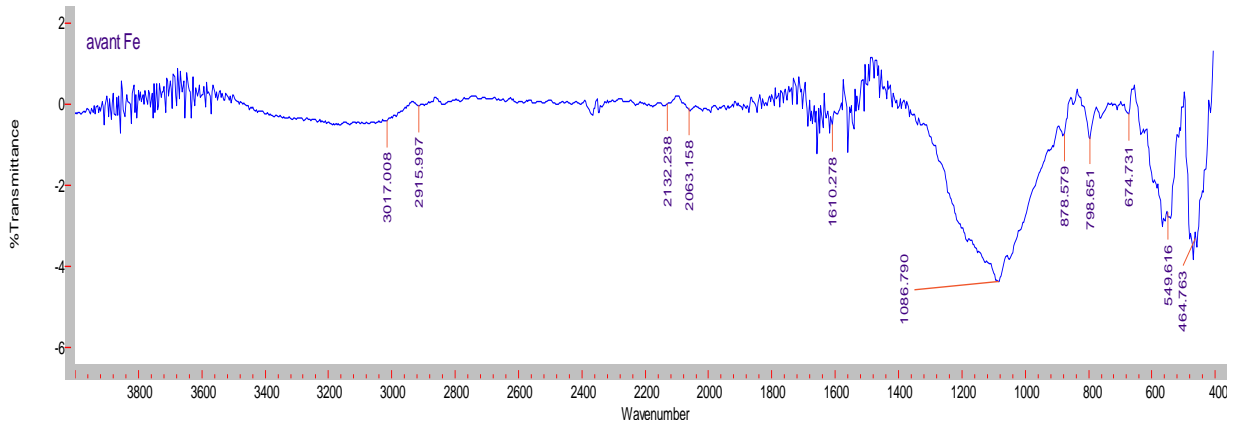
For the third trial, solution (S2) was prepared by mixing 8g of coagulant with 100ml of distilled water at a temperature of 90°C, with agitation until a viscous solution was obtained. Then, the same process as in step 2 was followed, except that

powdered activated charcoal was replaced with activated charcoal grains containing A (iron), B (silica), C (zinc), D (aluminum), and E (kaolin) for manufacturing the filter discs. The pellet press was not used; instead, the empty pellets were filled and left to dry for 1 hour. Although good results were obtained, they were not very conclusive.

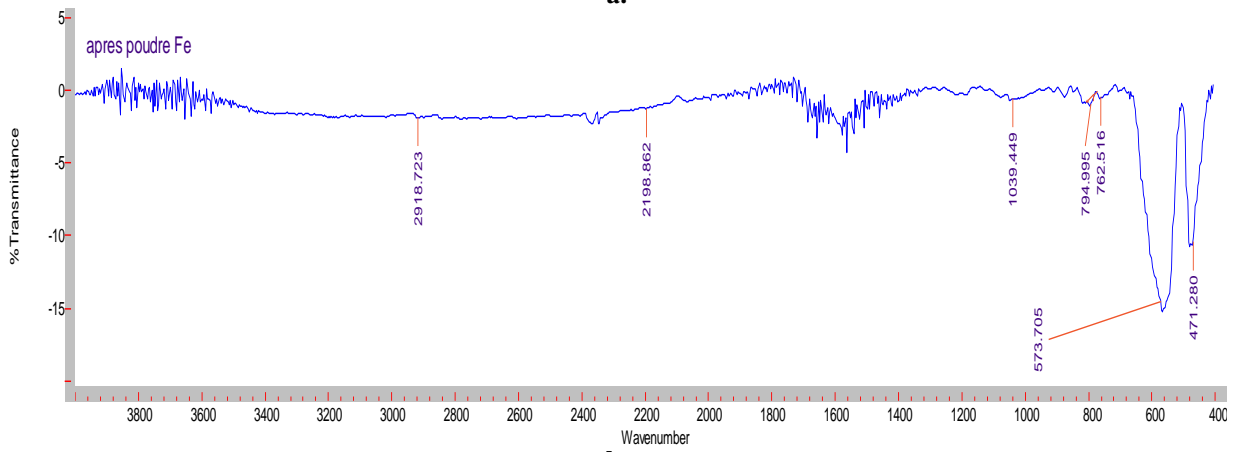
For the fourth trial, three mixed filter discs were prepared, consisting of 42.9% grain activated charcoal, 32.1% metal oxide, and 25% solution S2. These were placed in a mortar, ground to a paste, and then placed in the pellet press with a pressure of 20 tonnes. Subsequently, the pellets were placed in an oven to dry for 2 hours at a temperature of 90°C. The same steps were followed for the iron-based (FP1), zinc-based (FP2), and kaolin-based (FP3) filter discs. At the end of this experiment, it was observed that good results were obtained: these three discs met all the desired criteria, being robust with adequate permeability for the intended study.

3.2 Fourier transformed infrared (FTIR) test

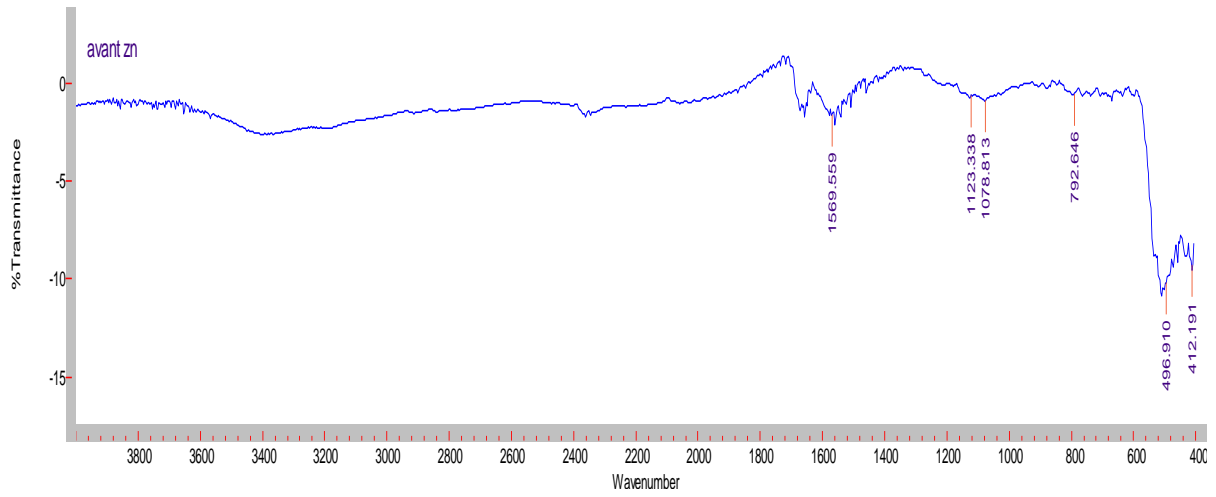
The infrared spectra of filter pellets (FP1, FP2, FP3) were compared before and after filtration by examining the literature data. The Figure 3a exhibited specific bands at wave numbers of 3354.17, 3194.65, 2933.67, 1663.44, 1047, and 526 cm^{-1} . These were identified as the stretching vibration modes of -C-NH₂ in -CONH₂ belonging to PAM, symmetrical stretching of -N-H in -CONH₂ associated with PAM, as well as the vibration modes of -CH₂ and -C=O [23]. The presence of amide is indicated by two characteristic absorption peaks located at 1318.06 and 1558.9 cm^{-1} , which represent the -COO- group and suggest the presence of acrylic monomers. The absence of -CH₃ in -N⁺(CH₃)₃ is reflected in the symmetric bending vibration absorption peak at 1451.60 cm^{-1} , while the symmetric vibration at 1414.54 cm^{-1} corresponds to N-CH₃. An intense band was discovered at 1086 cm^{-1} , which is linked to the symmetric stretching mode of the FeOOH functional group. Additionally, an average intensity band was observed at 878 cm^{-1} , which is attributed to the swinging mode of the FeOOH functional group. in the range of 600-400 cm^{-1} is associated with the stretching vibration of the Fe-O bond in the iron oxide structure. The Fe₂O₃ group is linked to the two intense peaks located at 573 cm^{-1} and 473 cm^{-1} which correspond to its rocking mode [24, 25]. By comparing Figure 3a to Figure 3b, we can observe changes in the infrared spectra of the FP1 sample. Specifically, we can note the absence of the band at 1083 cm^{-1} and an enhancement in the intensities of the absorption bands located at 573 cm^{-1} and 471 cm^{-1} . The prominent absorption band at 498 cm^{-1} seen in Figure 3c is attributed to the symmetric stretching mode of the Zn-O bond [26]. whereas the other absorption bands, which are not as distinct, are assigned to the amide functional group. After filtering the heavy metal solution, there was a small alteration observed in the intensities of the infrared bands in the FP2 spectrum figure. The kaolin sample showed two low intensity bands at 3691 cm^{-1} and 3618 cm^{-1} , which were attributed to the symmetrical elongation mode of the Al-O-H bond. In addition, high intensity bands were observed at 1093 cm^{-1} and 1037 cm^{-1} , which were attributed to the symmetrical and non-symmetrical stretching vibration of the Si-O bond. The SiO binding vibration of quartz was represented by a band of average intensity at 682 cm^{-1} . Finally, a band at 523 cm^{-1} was observed, which belonged to the non-symmetrical stretching vibration mode of the [27].



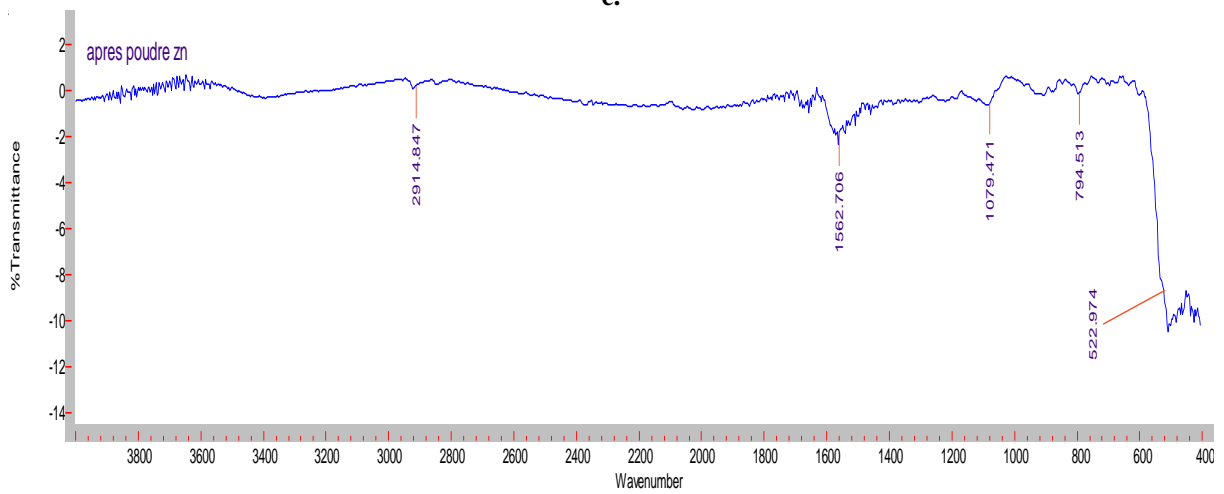
a.



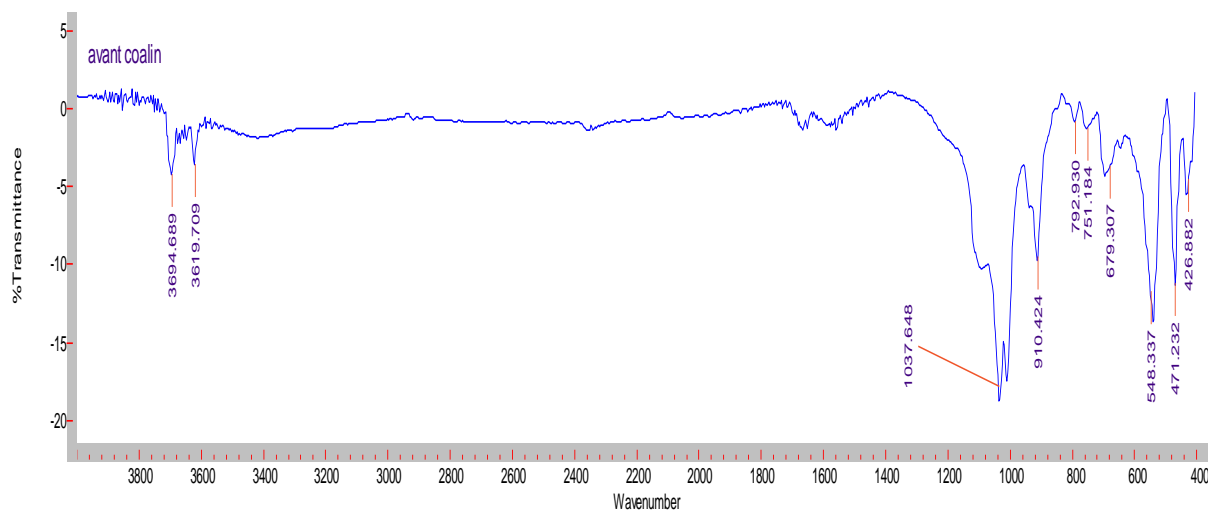
b.



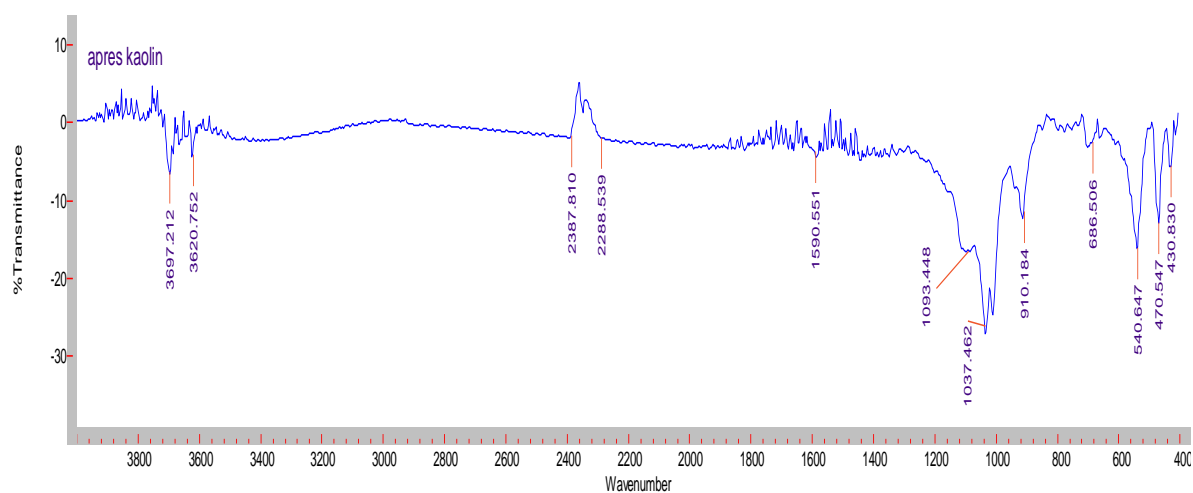
c.



d.



e.



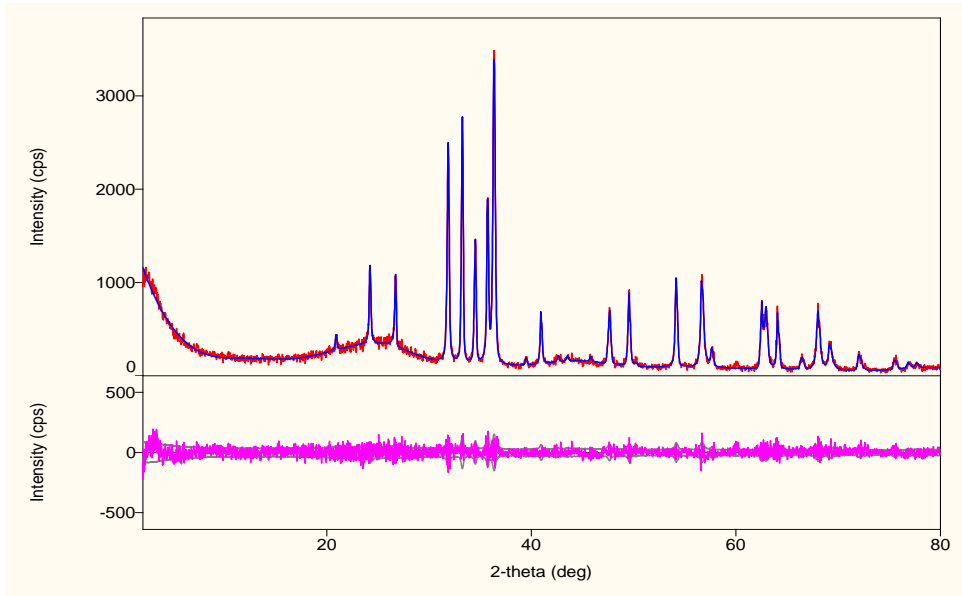
f.

Figure 3. a: FTIR spectrum of filter pellet (FP1) before retention of Ni(II) and Cr(VI) **b:** FTIR spectrum of filter pellet (FP1) after retention of Ni(II) and Cr(VI) **c:** FTIR spectrum of (FP2) before retention of Ni(II) and Cr(VI) **d:** FTIR spectrum of Filters pellets (FP2) after retention of Ni(II) and Cr(VI) **e:** FTIR spectrum of Filters pellets (FP3) before retention of Ni(II) and Cr(VI) **f:** FTIR spectrum of Filters pellets (FP3) before retention of Ni(II) and Cr(VI)

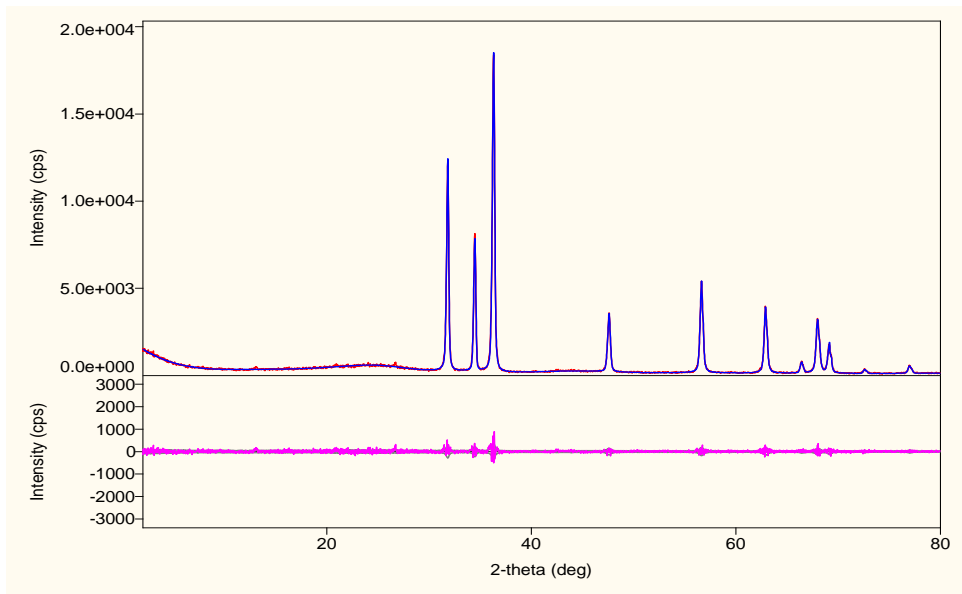
3.3 XRD patterns analysis

According to the literature, PAM has a structure that is amorphous in nature [28]. By examining Figures 4a, 4b, 4c, 4d, 4e and 4f The XRD pattern of activated carbon may also show a broad peak around $2\theta=43^\circ$, which corresponds to the (002) reflection of graphitic carbon [29]. This peak is usually very broad, indicating that the graphitic domains in the activated it is evident that there is a notable lack of peaks, particularly those that correspond to the diffraction angles 24.2° , 33.1° , 35.7° , 40.9° , 49.5° , 54.1° , 57.6° , 62.5° , 64.1° , 71.9° and 75.5° respectively pertaining to the planes of symmetry (012), (104), (110), (113), (024), (116), (018), (214), (300), (101) and (220) as determined by the diffractogram of $\alpha\text{-Fe}_2\text{O}_3$ (Hematite). Hematite is a common form with rhombohedral crystal structure [30]. The contrast between Figure 4a and Figure 4b indicates that the peaks located at 35.7° (110), 49.5° (024), and 71.9° (101) have vanished. This provides compelling evidence that the Cr(VI) and Ni(II) adsorbed have a discernible impact on the atomic positions within the iron oxide crystal, which is corroborated by the findings of the infrared spectroscopy analyses. Based on the literature's XRD pattern data for ZnO, it can be

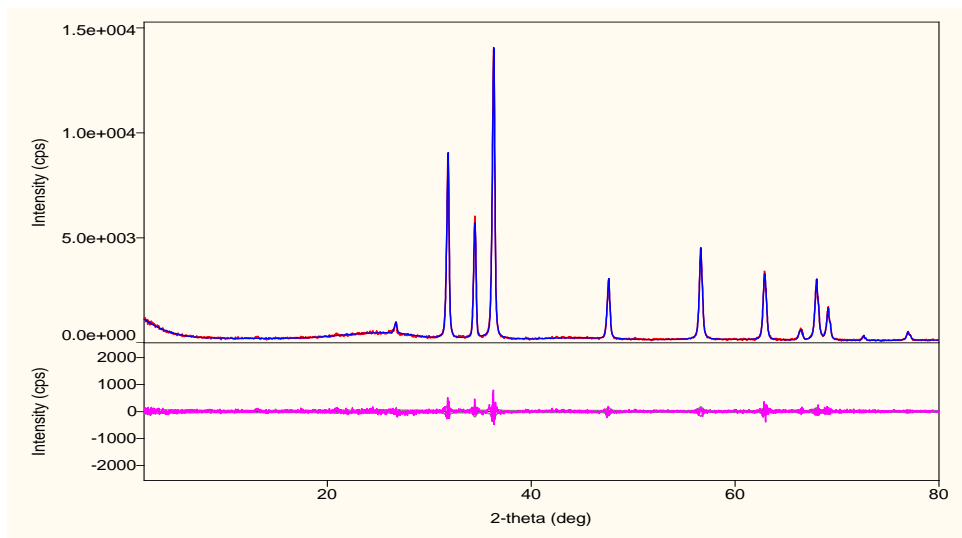
observed from Figure 4c that the peaks at 31.7° , 34.2° , 47.6° , 56.5° , 62.8° , 67.8° , 68.3° and 68.9° correspond to the crystal planes (100), (002), (101), (102), (110), (103), (200), (112) and (201) respectively [31]. By examining the XRD patterns in Figures 4c and Figure 4d, it can be observed that identical peaks are present in both diffractograms, indicating that the atomic arrangement of Crystal ZnO remains undisturbed when Cr(VI) and Ni(II) are juxtaposed with the FP2 sample, Which proves that the atomic positions of the atomic positions are not affected by the adsorption of Cr(VI) and Ni(II). By comparing the XRD pattern of kaolin to literature data, the peaks in Figure 4e were identified, with those at 2θ angles of 12.5° and 20.9° corresponding to the (001) and (002) crystal planes of the mineral [32]. The interaction of Cr(VI) and Ni(II) with the mineral affects the position of certain atoms and alters the planes of symmetry, as shown in Figure 4e and Figure 4f. While most of the peaks in the XRD analysis of the FP3 sample match the crystalline structure of kaolin, there are some differences from existing literature. Specifically, the filtered FP3 sample has an additional peak at a diffraction angle of 5° and 26.5° , and the peak at 27° is reduced.



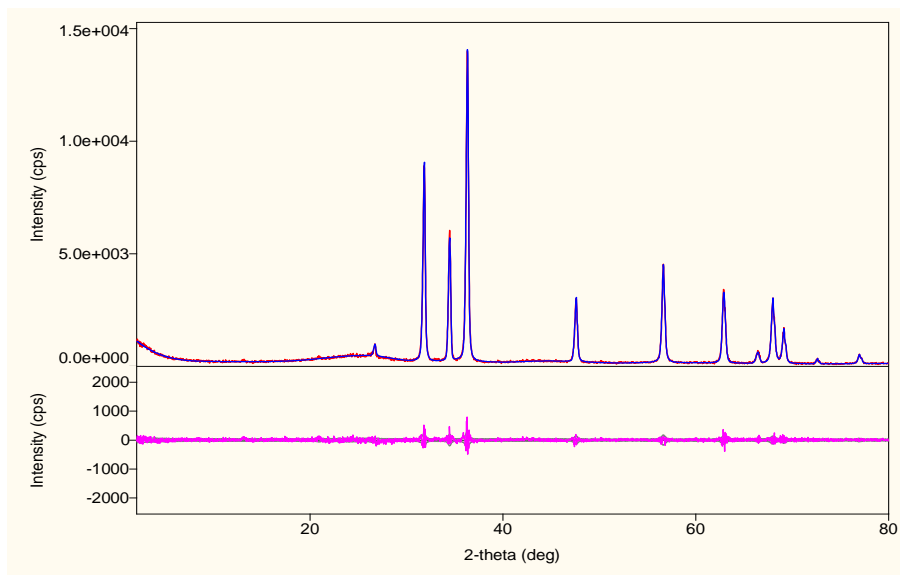
a



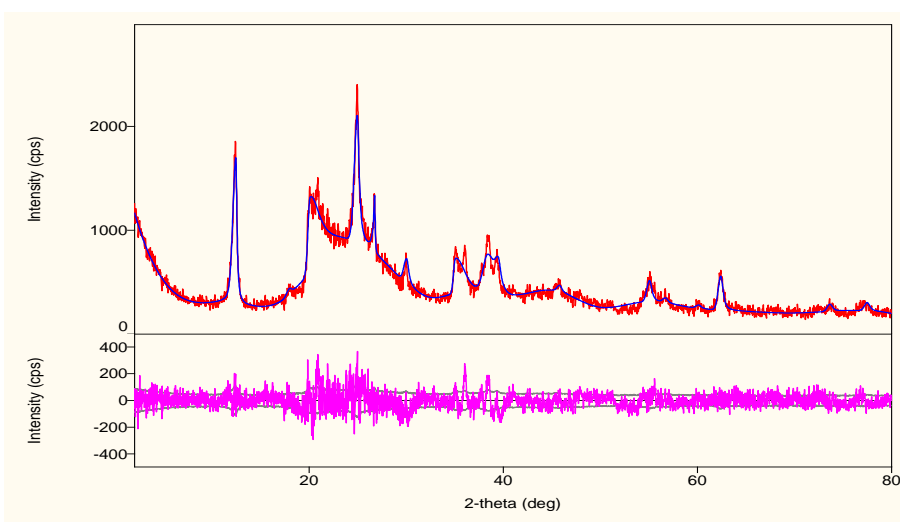
b



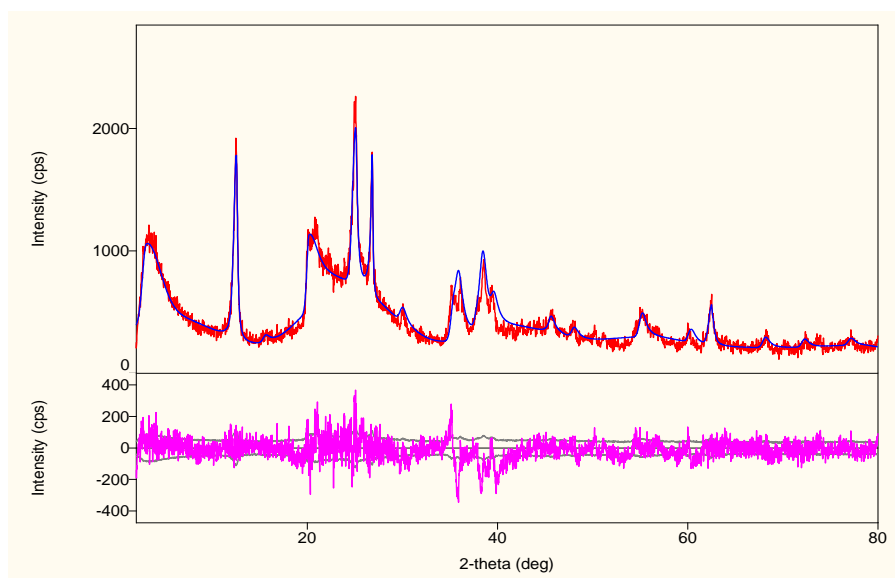
c



d



e



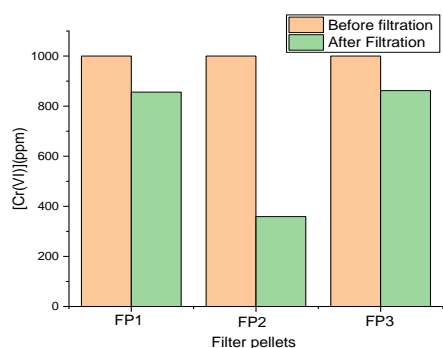
f

Figure 4. a: XRD pattern of Filters pellets (FP1) before retention of Ni(II) and Cr(VI) **b:** XRD pattern of Filters pellets (FP1) after retention of Ni(II) and Cr(VI) **c:** XRD pattern of Filter pellet (FP2) before retention of Ni(II) and Cr(VI) **d:** XRD pattern of Filter pellet (FP2) after retention of Ni(II) and Cr(VI) **e:** XRD pattern of Filter pellet (FP3) before retention of Ni(II) and Cr(VI) **f:** XRD pattern of Filter pellet (FP3) before retention of Ni(II) and Cr(VI)

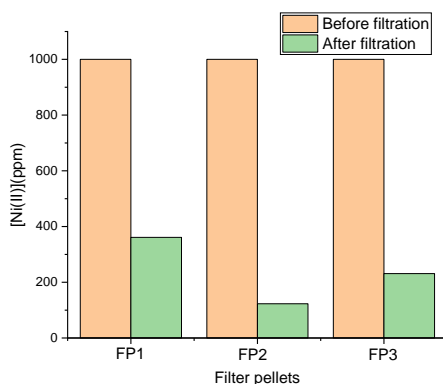
The X-ray diffraction (XRD) pattern of kaolin displays distinct peaks at 2θ angles of 12.5° , 20.9° , 24.7° , and 26.5° , corresponding to the (001), (002), (003), and (004) crystal planes of the mineral. The (001) peak, the narrowest and most intense peak, is used to determine the basal spacing of kaolin, which is typically around 7.2 \AA . The heavy metal interaction has an effect on the position of certain atoms and modifies the planes of symmetry of the kaolin mineral, as evidenced by the results presented in Figure 4e and Figure 4f. The XRD analysis of the FP3 sample shows that most of the peaks are in agreement with the crystalline structure of kaolin, but there are some differences between certain peaks when compared with existing literature. Specifically, the filtered FP3 sample exhibits an additional peak at a diffraction angle of 5° and 26.5° , while the peak at 27° is reduced in height.

3.4 XRF test

The Cr(VI) and Ni(II) retained by filter pellets were analyzed using XRF after being subjected to retention with initial concentration of Cr and Ni (100 ppm). Based on the findings shown in Figure 5a and Figure 5b it was discovered that filter pellets have a higher retention rate for Cr(VI) than Ni(II) ions. When comparing the retention efficiency of Cr(VI) and Ni(II) ions for each filter pellet, it was observed that filter pellet FP2 with ZnO additive had relatively low retention rates for Cr(VI) (35.9%) and Ni(II) (12.3%) compared to filter pellet FP1 with Fe_2O_3 additive and FP3 with Kaolin additive. On the other hand, the filter pellet FP3 containing Kaolin additive showed a retention rate of 86.2% for Cr(VI) and 23.1% for Ni(II) ions, while the filter pellet FP1 based on Fe_2O_3 had a retention rate of 85.6% for Cr(VI) ions and 36.1% for Ni(II) ions.



a



b

Figure 5. a: Efficiency of filter pellets in removing of Cr(VI)
b: Efficiency of filter pellets in removing of Ni(II)

3.5 Evaluations of ions retention by filter pellets

The conductimetric method is used in water treatment and environmental monitoring to assess water quality and pollutant levels. It measures conductivity to determine the presence of dissolved ions, which helps evaluate water hardness and quality [33]. The conductivity of the water decreased significantly after filtration, indicating the removal of the metals from the water. The results of ions retention by filter pellets using conductimetric method have shown the higher values retention rates of ions of FP1 and FP3 compared to FP2. This finding is of significant importance, as it suggests that FP1 and FP3 may be more effective in removing harmful ions from a given solution. Furthermore, these results are strongly related to the retention of chromium and nickel, as measured by XRF data. The high retention of ions by FP1 and FP3 may be the reason for their effectiveness in removing these particular heavy metals. This information is crucial in designing effective filtration systems for industrial processes, particularly those involving the removal of heavy metals from wastewater.

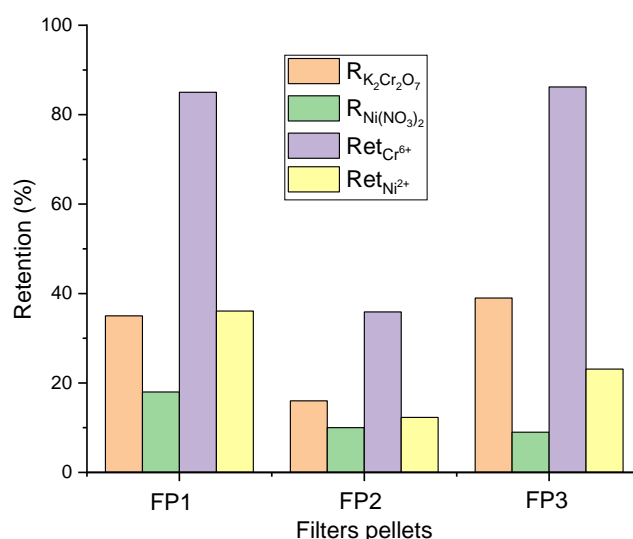


Figure 6. Compare ions retention: conductimetric vs. XRF on filter pellets for Cr^{6+} and Ni^{2+}

3.6 Comparative analysis

Cost analysis is an essential aspect in evaluating the feasibility of any new water treatment method, including filtration granules. The cost effectiveness of the new technology can be determined through a variety of factors, including maintenance requirements and the overall effectiveness of the treatment method in removing pollutants. When comparing the cost effectiveness of filtration granules to current water treatment methods, in cases where the water source is highly contaminated, filtration granules may provide a more cost-effective solution than traditional methods such as chemical treatment or reverse osmosis [34, 35]. They can effectively remove a wide range of pollutants with relatively low initial investment and minimal maintenance requirements. Additionally, filtration granules may provide a more sustainable and environmentally friendly alternative to traditional water treatment methods, as they do not require the use of chemicals or energy-intensive processes [36].

4. CONCLUSIONS

The preparation of new filter pellets based on PAM, GAC, ZnO, and kaolin, along with their application for water treatment, has shown promising results in the removal of Cr(VI) and Ni(II). The addition of iron oxide or kaolin additives to the filter pellets has been found to provide higher rejection rates for Cr(VI) and Ni(II) as compared to the filter pellets containing ZnO additives with low rejection rates of Cr(VI) and Ni(II). The comparison of retention efficiency between Cr(VI) and Ni(II) ions across the different filter pellets reveals intriguing insights. Filter pellet FP2, incorporating ZnO additive, demonstrated notably lower retention rates for Cr(VI) (35.9%) and Ni(II) (12.3%) in contrast to FP1 with Fe₂O₃ additive and FP3 with Kaolin additive. Conversely, FP3, enriched with Kaolin, exhibited impressive retention rates of 86.2% for Cr(VI) and 23.1% for Ni(II), while FP1, utilizing Fe₂O₃, showcased retention rates of 85.6% for Cr(VI) ions and 36.1% for Ni(II) ions. This has been confirmed through FTIR and XRD pattern comparisons, as well as the evaluation of retention tests using XRF data analysis and conductimetric results. These findings suggest that the new filter pellets have great potential for use in water treatment applications and can contribute to the development of more effective and efficient water treatment systems.

ACKNOWLEDGMENT

We would like to acknowledge the laboratory of spectrochemistry and structural pharmacology at the University of Tlemcen for providing the necessary resources and facilities to carry out this experimental work. We are grateful for the assistance provided by the lab staff during the course of this study. We would also like to express our appreciation to all those who contributed to this work in various ways. Without their help and support, this study would not have been possible.

REFERENCES

- [1] Zamora-Ledezma, C., Negrete-Bolagay, D., Figueroa, F., Zamora-Ledezma, E., Ni, M., Alexis, F., Guerrero, V.H. (2021). Heavy metal water pollution: A fresh look about hazards, novel and conventional remediation methods. *Environmental Technology and Innovation*, 22: 101504. <https://doi.org/10.1016/j.eti.2021.101504>
- [2] Briffa, J., Sinagra, E., Blundell, R. (2020). Heavy metal pollution in the environment and their toxicological effects on humans. *Heliyon*, 6(9): e04691. <https://doi.org/10.1016/j.heliyon.2020.e04691>
- [3] Ali, H., Khan, E., Ilahi, I. (2019). Environmental chemistry and ecotoxicology of hazardous heavy metals: Environmental persistence, toxicity, and bioaccumulation. *Journal of Chemistry*, 2019: 6730305. <https://doi.org/10.1155/2019/6730305>
- [4] DesMarias, T.L., Costa, M. (2019). Mechanisms of chromium-induced toxicity. *Current Opinion in Toxicology*, 14: 1-7. <https://doi.org/10.1016/j.cotox.2019.05.003>
- [5] Genchi, G., Carocci, A., Lauria, G., Sinicropi, M.S., Catalano, A. (2020). Nickel: Human health and environmental toxicology. *International Journal of Environmental Research and Public Health*, 17(3): 679. <https://doi.org/10.3390/ijerph17030679>
- [6] Ng, N.T., Kamaruddin, A.F., Wan Ibrahim, W.A., Sanagi, M.M., Abdul Keyon, A.S. (2017). Advances in organic-inorganic hybrid sorbents for the extraction of organic and inorganic pollutants in different types of food and environmental samples. *Journal of Separation Science*, 41(1): 195-208. <https://doi.org/10.1002/jssc.201700689>
- [7] Gil, A., Santamaria, L., Korili, S.A., Vicente, M.A., Barbosa, L.V., de Souza, S.D., Ciuffi, K.J. (2021). A review of organic-inorganic hybrid clay based adsorbents for contaminants removal: Synthesis, perspectives and applications. *Journal of Environmental Chemical Engineering*, 9(5): 105808. <https://doi.org/10.1016/j.jece.2021.105808>
- [8] Kumar, M., Sharma, A., Maurya, I.K., Thakur, A., Kumar, S. (2019). Synthesis of ultra small iron oxide and doped iron oxide nanostructures and their antimicrobial activities. *Journal of Taibah University for Science*, 13(1): 280-285. <https://doi.org/10.1080/16583655.2019.156543>
- [9] Krishnamoorthy, R., Sagadevan, V. (2015). Polyethylene glycol and iron oxide nanoparticles blended polyethersulfone ultrafiltration membrane for enhanced performance in dye removal studies. *e-Polymers*, 15(3): 151-159. <https://doi.org/10.1515/epoly-2014-0214>
- [10] Shen, L., Huang, Z., Liu, Y., Li, R., Xu, Y., Jakaj, G., Lin, H. (2020). Polymeric membranes incorporated with ZnO nanoparticles for membrane fouling mitigation: A brief review. *Frontiers in Chemistry*, 8: 224. <https://doi.org/10.3389/fchem.2020.00224>
- [11] Zhu, W., Wang, J., Wu, D., Li, X., Luo, Y., Han, C., He, S. (2017). Investigating the heavy metal adsorption of mesoporous silica materials prepared by microwave synthesis. *Nanoscale Research Letters*, 12(1): 1-9. <https://doi.org/10.1186/s11671-017-2070-4>
- [12] Chen, M., Yang, T., Han, J., Zhang, Y., Zhao, L., Zhao, J., Li, R., Huang, Y., Gu, Z., Wu, J. (2023). The application of mineral kaolinite for environment decontamination: A review. *Catalysts*, 13(1): 123. <https://doi.org/10.3390/catal13010123>
- [13] Abdulrazak, S., Hussaini, K. Sani, H.M. (2017). Evaluation of removal efficiency of heavy metals by low-cost activated carbon prepared from African palm fruit. *Applied Water Science*, 7: 3151-3155. <https://doi.org/10.1007/s13201-016-0460>
- [14] Jjagwe, J., Olupot, P.W., Menya, E., Kalibbala, H.M. (2021). Synthesis and application of Granular activated carbon from biomass waste materials for water treatment: A review. *Journal of Bioresources and Bioproducts*, 6(4): 292-322. <https://doi.org/10.1016/j.jobab.2021.03.003>
- [15] Hou, T., Yu, S., Zhou, M., Wu, M., Liu, J., Zheng, X., Wang, X. (2020). Effective removal of inorganic and organic heavy metal pollutants with poly (amino acid)-based micromotors. *Nanoscale*, 12(8): 5227-5232. <https://doi.org/10.3390/polym15030500>
- [16] Brunel, D.G., Pachekoski, W.M., Dalmolin, C., Agnelli, J.A.M. (2014). Natural additives for poly (hydroxybutyrate-CO-hydroxyvalerate)-PHBV: Effect on mechanical properties and biodegradation. *Materials*

- Research, 17(5): 1145–1156. <https://doi.org/10.1021/acsomega.9b00981>
- [17] Park, J., Park, J., Park, J., Kim, H., Jeong, Y. (2007). Preparation and characterization of porous cordierite pellets and use as a diesel particulate filter. *Separation and Purification Technology*, 55(3): 321–326. <https://doi.org/10.1016/j.seppur.2006.11.009>
- [18] Hoslett, J., Massara, T.M., Malamis, S., Ahmad, D., van den Boogaert, I., Katsou, E., Jouhara, H. (2018). Surface water filtration using granular media and membranes: A review. *Science of The Total Environment*, 639: 1268–1282. <https://doi.org/10.1016/j.scitotenv.2018.05.2>
- [19] Daou, I., Lecomte-Nana, G., Tessier-Doyen, N., Peyratout, C., Gonon, M., Guinebretiere, R. (2020). Probing the dehydroxylation of kaolinite and halloysite by in situ high temperature X-ray diffraction. *Minerals*, 10(5): 480. <https://doi.org/10.1590/1516-1439.235613>
- [20] Costa, S.M., Fowler, D., Carreira, G.A., Portugal, I., Silva, C.M. (2022). Production and upgrading of recovered carbon black from the pyrolysis of end-of-life tires. *Materials*, 15(6): 2030. <https://doi.org/10.3390/ma15062030>
- [21] Chabane, M., Melkaoui, C., Dahmani, B., Belalia, S.Z. (2020). Preparation and characterization of matrix hybrid membranes polyvinylidene fluoride/polyvinylpyrrolidone/silica gel/zinc oxide for Cr(VI) removal from water. *Annales de Chimie - Science des Matériaux*, 44(5): 311-318. <https://doi.org/10.18280/acsm.440502>
- [22] Ademiluyi, F.T., David-West, E.O. (2012). Effect of chemical activation on the adsorption of heavy metals using activated carbons from waste materials. *International Scholarly Research Notices*, 2012: 674209. <https://doi.org/10.5402/2012/674209>
- [23] Chen, Z.Y., Gao, S., Zhou, R.B., Wang, R.D., Zhou, F. (2022). Dual-crosslinked networks of superior stretchability and toughness polyacrylamide-carboxymethylcellulose hydrogel for delivery of alendronate. *Materials & Design*, 217: 110627. <https://doi.org/10.1016/j.matdes.2022.110627>
- [24] Bozkurt, G. (2020). Synthesis and characterization of α -Fe₂O₃ nanoparticles by microemulsion method. *Erzincan University Journal of Science and Technology*, 13(2): 890-897. <https://doi.org/10.18185/erzifbed.742160>
- [25] Mohandoss, N., Renganathan, S., Subramaniyan, V., Nagarajan, P., Elavarasan, V., Subramaniyan, P., Vijayakumar, S. (2022). Investigation of biofabricated iron oxide nanoparticles for antimicrobial and anticancer efficiencies. *Applied Sciences*, 12(24): 12986. <https://doi.org/10.3390/app12241298>
- [26] Sowri Babu, K., Ramachandra Reddy, A., Sujatha, C., Venugopal Reddy, K., Mallika, A.N. (2013). Synthesis and optical characterization of porous ZnO. *Journal of Advanced Ceramics*, 2(3): 260-265. <https://doi.org/10.1007/s40145-013>
- [27] Otieno, S., Kowenje, C., Kengara, F., Mokaya, R. (2021). Effect of kaolin pre-treatment method and NaOH levels on the structure and properties of kaolin-derived faujasite zeolites. *Materials Advances*, 2(18): 5997-6010. <https://doi.org/10.1039/d1ma00449b>
- [28] Tarasova, N., Zanin, A., Krivoborodov, E., Toropygin, I., Pascal, E., Mezhev, Y. (2021). The new approach to the preparation of polyacrylamide-based hydrogels: Initiation of polymerization of acrylamide with 1, 3-dimethylimidazolium (phosphonoxy-) oligosulphanide under drying aqueous solutions. *Polymers*, 13(11): 1806. <https://doi.org/10.3390/polym13111806>
- [29] Kielbasa, K., Bayar, Ş., Varol, E.A., Sreńscek-Nazzal, J., Bosacka, M., Miądlicki, P., Serafin, J., Wróbel, R.J., Michalkiewicz, B. (2022). Carbon dioxide adsorption over activated carbons produced from molasses using H₂SO₄, H₃PO₄, HCl, NaOH, and KOH as activating agents. *Molecules*, 27(21): 7467. <https://doi.org/10.3390/molecules27217467>
- [30] Baabu, P.R.S., Kumar, H.K., Gumpu, M.B., Babu K.J., Kulandaisamy, A.J., Rayappan, J.B.B. (2022). Iron oxide nanoparticles: A review on the province of its compounds, properties and biological applications. *Materials*, 16(1): 59. <https://doi.org/10.3390/ma16010059>
- [31] Grande-Tovar, C.D., Castro, J.I., Valencia Llano, C.H., Tenorio, D.L., Saavedra, M., Zapata, P.A., Chaur, M.N. (2022). Polycaprolactone (PCL)-polylactic acid (PLA)-glycerol (Gly) composites incorporated with zinc oxide nanoparticles (ZnO-NPs) and tea tree essential oil (TTEO) for tissue engineering applications. *Pharmaceutics*, 15(1): 43. <https://doi.org/10.3390/pharmaceutics15010043>
- [32] Fang, C., Veiseh, O., Kievit, F., Bhattacharai, N., Wang, F., Stephen, Z., Zhang, M. (2010). Functionalization of iron oxide magnetic nanoparticles with targeting ligands: Their physicochemical properties and in vivo behavior. *Nanomedicine*, 5(9): 13571369. <https://doi.org/10.2217/nnm.10.55>
- [33] Afkhami, A., Marotta, M., Dixon, D., Ternan, N.G., Montoya-Jaramillo, L.J., Hincapie, M., Dunlop, P.S.M. (2020). Assessment of low-cost cartridge filters for implementation in household drinking water treatment systems. *Journal of Water Process Engineering*, 2020: 101710. <https://doi.org/10.1016/j.jwpe.2020.101710>
- [34] Abushawish, A., Bouaziz, I., Almanassra, I.W., AL-Rajabi, M.M., Jaber, L., Khalil, A.K., Takriff, M.S., Laoui, T., Shanableh, A., Atieh, M.A., Chatla, A. (2023). Desalination pretreatment technologies: Current status and future developments. *Water*, 15(8): 1572. <https://doi.org/10.3390/w15081572>
- [35] Lahnafi, A., Elgamouz, A., Tijani, N., Shehadi, I. (2020). Hydrothermal synthesis of zeolite A and Y membrane layers on clay flat disc support and their potential use in the decontamination of water polluted with toxic heavy metals. *Desalination and Water Treatment*, 182: 175–186. <https://doi.org/10.5004/dwt.2020.25173>
- [36] Tran, T.P.A., Cho, H., Cho, G.C., Han, J.I., Chang, I. (2021). Nickel (Ni²⁺) removal from water using gellan gum–sand mixture as a filter material. *Applied Sciences*, 11(17): 7884. <https://doi.org/10.3390/app11177884>

NOMENCLATURE

PAM	Polyacrylmaide
GAC	Granuled active carbon
BO(%)	Burn of percentage
C_{Ads}	Concentration of heavy metal adsorbed by filters pellets (ppm)

C_{Feed}	Concentration of heavy metal in feed solution (ppm)	XRF	X ray Fluorescence
R(%)	Rejection rate of filters pellets	XRD	X ray diffraction
Re(%)	Rejection rate of filters pellets (%)	WDXRF	Wavelength Dispersive X-ray Fluorescence Spectrometer
$\rho_{permeate}$	Conductivity of permeate solution ($\mu\text{s}/\text{cm}$)	CV	The precision of analysis
ρ_{Feed}	Conductivity of feed solution ($\mu\text{s}/\text{cm}$)		
FTIR	Fourier transformed infrared		